Density and Distribution of α-Bungarotoxin-binding Sites in Postsynaptic Structures of Regenerated Rat Skeletal Muscle

DAVID BADER

Department of Anatomy, University of Michigan Medical School, Ann Arbor, Michigan 48109. Dr. Bader's present address is the Department of Anatomy, State University of New York, Downstate Medical Center, Brooklyn, New York 11203.

ABSTRACT Acetylcholine receptors (AChR) are organized in a discrete and predictable fashion in the postsynaptic regions of vertebrate skeletal muscle. When muscle is damaged, nerves and myofibers including muscular elements of the endplate degenerate, but the connective tissue elements survive. Muscle fibers regenerate within the basal lamina of the original myofiber. Postsynaptic differentiation in regenerated mammalian skeletal muscle can occur in different ways: (*a*) at the site of the original endplate in the presence or absence of the nerve, or (*b*) at ectopic regions of the regenerated myofiber in the presence of the nerve when the original endplate is not present. The present study used ^{125}I-α-bungarotoxin (^{125}I-α-BuTX) and EM autoradiography to examine the density and distribution of AChR in postsynaptic structures regenerated at the site of the original endplate in the absence of the nerve and at ectopic sites of the myofiber in the presence of the nerve when the original endplate was removed. In regenerated myofibers, the density of α-BuTX-binding sites fell within the range of densities observed in uninjured muscle whether postsynaptic differentiation occurred at the site of the original endplate in the absence of the nerve or at an originally ectopic position of the regenerated myofiber. In addition, the distribution of α-BuTX-binding sites within the regenerated postsynaptic regions closely resembled the distribution of α-BuTX-binding sites in uninjured muscle. Morphometric analysis was performed on postsynaptic structures formed at the site of the original endplate in the absence of the nerve or at an ectopic position of the regenerated myofiber by interaction of the nerve and muscle. Although variation in the depth of the primary cleft occurred, there was little difference between the overall structure of regenerated postsynaptic structures and that of endplates of uninjured muscles.

The density of acetylcholine receptors (AChR) at innervated motor endplates of skeletal muscle has been determined by both physiological (23, 25) and morphological (16, 28, 30, 33–35) means. Various studies (for review see reference 12) have shown that the number of AChR at endplates in mice (2), rats (14, 31), frogs (31), and humans (13) is quite similar. Electron microscope autoradiographic studies have demonstrated a relatively constant density (16, 28, 30, 33–35) and distribution (16, 33–35) of AChR at endplates of vertebrate skeletal muscle.

When skeletal muscle grafts are made, the neuromuscular junctions are disrupted by the degeneration of the myofibers and the nerves that supply them (7, 10, 29, 37, and footnote 1). It has been established that synapses are formed in the regenerated muscle of amphibians (29, 37) and mammals (1, 3, 10). Marshall et al. (29) have shown that, in regenerating frog muscle, neuromuscular connections are almost always at the site of the original endplate. Burden et al. (7) have demonstrated that postsynaptic differentiation, including accumulation of AChR to levels observed in normally innervated endplates, occurs at the site of the original motor endplate in regenerated frog skeletal muscle, even in the absence of the nerve. Recent studies of mammalian skeletal muscle regener-

[1] Carlson, B. M., P. Hnik, S. Tucek, R. Vejsada, and D. Bader. Comparison between standard free muscle grafts and grafts with intact nerves in the rat EDL muscle. Manuscript in preparation.

THE JOURNAL OF CELL BIOLOGY · VOLUME 88 FEBRUARY 1981 338-345

ation (1, 38) have determined that the presence of the original endplate region is essential for the overall success of the muscle graft. New endplates are formed in grafts devoid of original endplates but they are few in number when compared with the number of endplates formed in muscle grafts when original endplates are present (1).

From these previous studies of skeletal muscle regeneration, it is apparent that postsynaptic differentiation in damaged muscle can occur in different ways. It is also apparent from previous EM autoradiographic studies that a relatively constant density and distribution of AChR are observed in endplates of mammalian skeletal muscle. The present study examined postsynaptic structures in regenerating rat skeletal muscle that differentiated in two different ways: (*a*) at the site of the original endplate in the absence of the nerve, and (*b*) at ectopic positions on the regenerated myofiber by interaction of the nerve and muscle when the original endplate was not present. EM autoradiography and ^{125}I-α-BuTX were used to examine the density and distribution of AChR in endplates regenerated in these two different ways. These experiments were conducted to determine whether postsynaptic structures derived in vastly different developmental processes would attain the arrangement of AChR observed in endplates of uninjured skeletal muscle.

MATERIALS AND METHODS

Purification and Iodination of α-BuTX

α-BuTX (purchased from Sigma Chemical, St. Louis, Mo.) was purified similar to the method of Berg et al. (5). Purified α-BuTX was labeled with ^{125}I (purchased from Amersham Corp., Arlington Heights, Ill.) by the chloramine-T method of Greenwood et al. (19). Four separate batches of ^{125}I-α-BuTX were prepared during this study, with specific activities ranging from 44 to 238 Ci/mmol. Specific activities of different batches of α-BuTX were determined from the ratio of radioactivity and protein concentrations. The molarity of ^{125}I-α-BuTX was determined by a Lowry protein assay using bovine serum albumin as a standard. The apparent protein concentration of the ^{125}I-α-BuTX was multiplied by a correction factor of 0.57 to obtain the correct specific activity of the radioactive compound (see reference 27 for details on determination of specific activity of ^{125}I-α-BuTX). In all cases, ^{125}I-α-BuTX was used within 10 d of preparation.

Control and Experimental Groups: Surgical Procedures

Male Sprague-Dawley rats (Charles River) that initially weighed 150–175 g were used in this study. Surgery was done under ether anesthesia. Muscles were exposed by cutting the overlying skin and fascia, and all suturing of tendons, fascia, and skin was done with surgical thread. All animals were kept under standard laboratory conditions. Unless otherwise stated, all muscles were poisoned with ^{125}I-α-BuTX at a concentration of 1.5×10^{-6} M in Kreb's solution (5) by topical application.

Innervated, Noninjured Muscle

For determination of the density of α-BuTX-binding sites in normal muscle, two extensor digitorum longus (EDL) muscles and two soleus (SOL) muscles were poisoned with ^{125}I-α-BuTX. The muscles were surgically exposed and the toxin was applied topically until there was total blockage of nerve-evoked tetanic muscle contraction. This was determined by stimulating the nerve to the muscle with hook electrodes every 20 min at a stimulating frequency of 100 Hz. Total blockage of tetanic response usually took <2.5 h.

Denervated, Noninjured Muscle

In two rats, the sciatic nerve was severed and reflected to totally denervate the hindlimb. 40 d after denervation, the SOL muscle was exposed and treated with ^{125}I-α-BuTX for 3 h.

Noninnervated, Regenerated Muscle Grafts with Original Motor Endplates

In three rats, the SOL was taken from its bed and cut into three pieces (Fig. 1). The three pieces were soaked in 0.75% Marcaine (Winthrop Laboratories, New York) for 10 min to insure the initial destruction of all grafted myofibers (9) and then grafted into the bed of the ablated EDL. Then the sciatic nerve, at the level of the sciatic notch, was severed and reflected to totally denervate the hindlimb. 40 d after surgery, the muscle grafts were isolated in the limb and poisoned with ^{125}I-α-BuTX for 3 h.

Muscle Grafts Devoid of Original Motor Endplates

Soleus muscles were removed from their muscle bed and cut into three segments (Fig. 1). The middle piece was tested histochemically for acetylcholinesterase (22) either as a whole mount or as serial sections cut in a cryostat to determine whether all original motor endplates were removed. As previously noted (1, 18, 20), the endplates of the rat soleus muscle are located only at the mid-portion of the muscle. All endplates were considered to be removed if the zone of acetylcholinesterase-positive motor endplates had a region of non-acetylcholinesterase-stained muscle on both sides of the motor endplate zone. The two aneural portions of the muscle were soaked in 0.75% Marcaine. The muscle graft was then placed in the bed of the EDL muscle after its ablation. No attempt was made to direct the cut nerve of the EDL to the muscle graft. The tendons of the muscle graft were sutured to the tendon stumps of the EDL. The grafts were allowed to regenerate for 60 d because it was felt that stable neuromuscular connections would be made by that time. 60 d after grafting, three such grafts were poisoned with ^{125}I-α-BuTX for 3 h. Muscle grafts devoid of original motor endplate do not undergo constant and predictable contraction after electrical stimulation to the nerve entering the muscle graft (1). A 3-h time period of toxin application was chosen because it was found that α-BuTX-binding sites were saturated during this time period (see below: "α-BuTX-binding Studies").

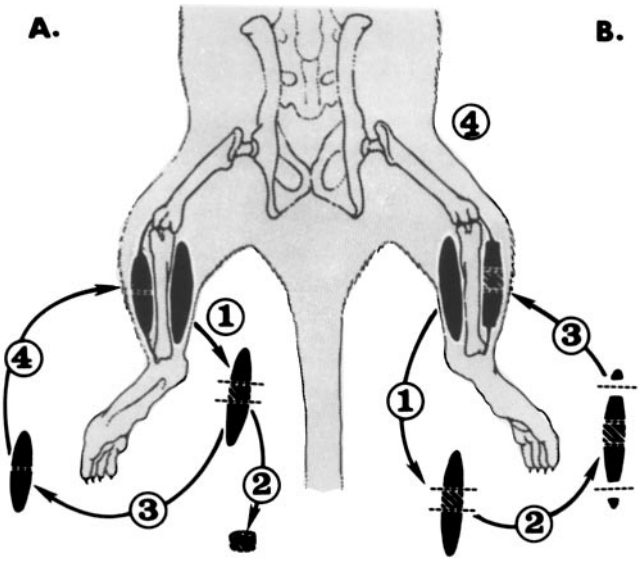

FIGURE 1 Experimental techniques used to produce muscle grafts. (*A*) Left side: Grafts devoid of original endplates. (*1*) The SOL muscle was taken from its bed and cut into three pieces. (*2*) The middle piece which contained the endplate zone was tested histochemically (24) for the complete removal of endplates. (*3*) The two remaining aneural portions of the muscle were then placed into the bed of the ablated EDL and (*4*) sutured to the tendons of the EDL. (*B*) Right side: Grafts with original endplates in denervated legs. (*1*) The SOL muscle was taken from its bed and cut into three pieces. (*2*) The three pieces were placed together and the ends of the muscle grafts were cut so that it would better fit the bed of the EDL. (3) The graft was placed in the bed of the ablated EDL and sutured to its tendons. (*4*) At the level of the sciatic notch, the sciatic nerve was cut and reflected to totally denervate the hindlimb. Similar to Fig. 1 of reference 1.

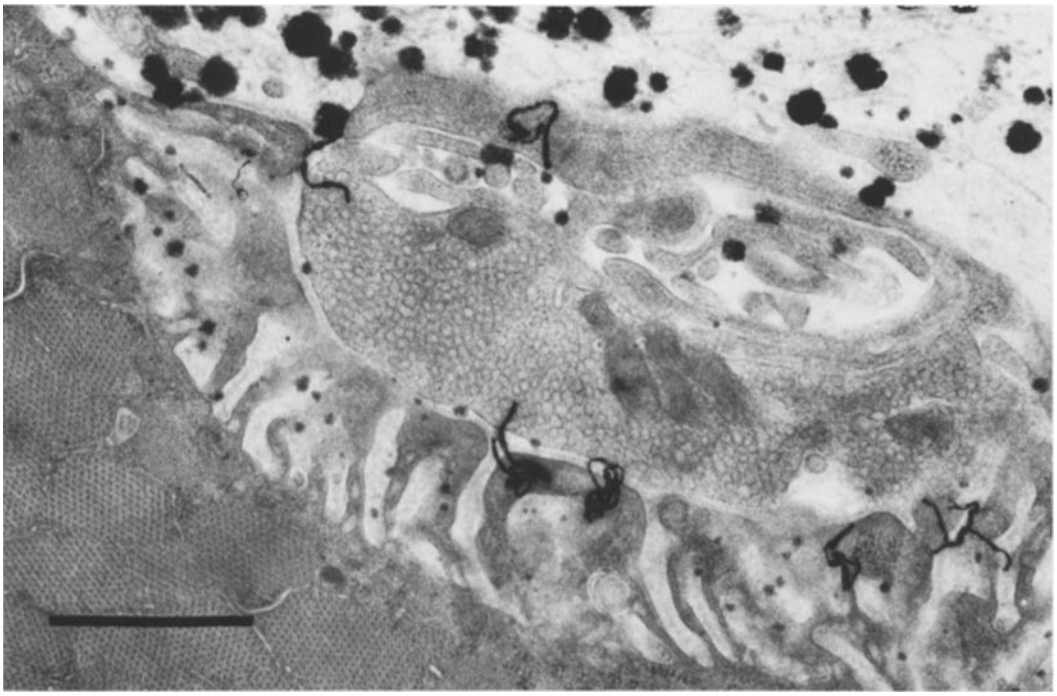

FIGURE 2 Autoradiogram of neuromuscular junction of uninjured EDL muscle. The overall structure of the endplate is characteristic of mammalian endplates (see text). This muscle was treated with ^{125}I-α-BuTX until tetanus was completely blocked. The α-BuTX-binding sites represented by the developed silver grains are associated with the top of the secondary cleft. The black precipitate is from acetylcholinesterase stain. Flat substrate technique, Microdol-X developer, uranyl acetate/lead citrate stain. Bar, 1.0 μm. × 26,000.

Tissue Preparation and Electron Microscope Autoradiography

1.5–2 h after the final application of α-BuTX, the muscles, either control or experimental, were fixed at resting muscle length in 2% glutaraldehyde in phosphate buffer for 2 h. The glutaraldehyde-fixed tissue was then treated with a stain for acetylcholinesterase (22) for 20 min. Regions that contained motor endplates were dissected out, postfixed in 1% osmium tetroxide in phosphate buffer for 1 h, and processed for electron microscopy with Epon 812/Araldite resins. Pale gold sections (100 nm ± 10% in thickness judged by interferometry) were cut and processed for electron microscope autoradiography. By use of either the loop technique (6) or the flat substrate technique (36), monolayers of Ilford L-4 emulsions were applied to the sections. No significant difference was observed in grain densities in sections from the same block by either technique. The autoradiograms were exposed for 1–8 wk and then developed with D-19 (2 min, 20°C) or Microdol-X (2 min, 25°C), fixed, and stained with uranyl acetate and lead citrate. All endplates in the sections were photographed in a Siemens 101 microscope at an initial magnification of 10,000.

Analysis of Autoradiograms

The determination of grain density (grains/micrometer^2) and of the length of primary and secondary clefts and the thickened postsynaptic membrane were determined by previously published morphometric procedures (15, 16). Histograms of the grain distribution in motor endplates were constructed for the various control and experimental groups. The center of all developed grains within 0.5 μm on the axonal side and 1.0 μm on the muscle side of the primary cleft was found, and the distance from this point to a line drawn over the crests of the junctional folds was measured. Grain density at different distances from the line drawn over the crests of the junctional folds was determined as described by Fertuck and Salpeter (16). The grain density was expressed in HDs (or half distance of exposed grains) from this line.[2]

α-BuTX-binding Studies

These experiments were conducted to insure that α-BuTX-binding sites were saturated during the period of α-BuTX application described above. Three separate batches of ^{125}I-α-BuTX were tested. For each batch of ^{125}I-α-BuTX, one rat soleus muscle was treated with nonradioactive α-BuTX at a concentration of 1.5×10^{-6} M for 3 h (blockage of neuronally induced tetanic response was always complete in 2.5 h). This was followed by treatment of the muscle with ^{125}I-α-BuTX for 2 h. Another SOL muscle was treated with ^{125}I-α-BuTX for 3 h. These six animals were maintained for 12–18 h before the muscles were removed and homogenized in buffer (Tris-Cl, 10 mM; NaCl, 50 mM; pH 7.4). This homogenate was centrifuged at 15,000 *g* for 30 min and the resulting pellet was resuspended in buffer containing Tris-Cl, 10 mM; NaCl, 50 mM; Triton X-100, 1%, pH 7.4. Three 120-μl aliquots of each homogenate were counted in a gamma counter.

When tetanus was blocked with ^{125}I-α-BuTX, the radioactivity of samples from these muscles was 28.3×10^3, 15.1×10^3, and 12.4×10^3 cpm for ^{125}I-α-BuTX batches 1–3, respectively.[3] When tetanus was blocked with nonradioactive α-BuTX, followed by ^{125}I-α-BuTX treatment, the radioactivity of samples was 1.1×10^3, 0.95×10^3, and 0.31×10^3 for ^{125}I-α-BuTX batches 1–3, respectively. This represents over a 90% drop in radioactivity when nonradioactive α-BuTX was used to block tetanus and indicates that α-BuTX-binding sites are essentially saturated during the first 3 h of toxin application.

RESULTS AND DISCUSSION

Uninjured EDL and SOL Muscles

The diameters of individual endplates as determined from AChE-stained cryostat sections of EDL and SOL muscles were 37 ± 16 and 34 ± 6 μm, respectively. In endplates of both the EDL and SOL muscles, the space between the pre- and postsynaptic membranes (50 nm) was always split by a basal lamina which also extended into the secondary cleft. The thickened postsynaptic membrane was found at the top of the junctional folds and extended down the sides of the folds ~200 nm. The depth of the secondary cleft was ~900 and ~870 nm in endplates of the EDL and SOL muscles, respectively. The bottom of the secondary clefts of endplates of the EDL muscle lay close to the outer surface of the myofibrils (Fig. 2), whereas

[2] HD or half distance is the distance in which half of all exposed grains from a linear radioactive source fall. In this case, with Ilford L4, ^{125}I and D19 developer, the HD value was determined to be ~80 nm.

[3] These values represent the average cpm (±10%) of the three aliquots from each muscle.

endplates of the SOL muscle had more cytoplasmic elements between the bottom of the clefts and the outermost myofibrils. Morphometric analysis of endplates in uninjured muscle is presented in Table I. The grain distribution over uninjured EDL endplates showed that the greatest concentration of α-BuTX sites was located in the 200-nm region near the crests of the junctional folds (Fig. 7) and that the grain density at the bottom of the folds was nearly the levels seen at extrajunctional regions. The presynaptic membrane may have up to 5% of the α-BuTX binding of the thickened postsynaptic membrane (30). Therefore it is assumed that the greatest share of the radioactivity seen at the interface of the pre- and postsynaptic membranes is caused by α-BuTX binding the postsynaptic membrane (see Table I for α-BuTX binding densities).

Denervated SOL Muscle

The diameter of motor endplates in 40-d denervated SOL muscle was 31 ± 8 μm, which was not significantly different from that of innervated SOL endplates. Although the diameter of the denervated muscle fibers was smaller than that of innervated SOL myofibers, the ultrastructure of the endplate generally resembled that of innervated endplates (Fig. 3). The depth of the secondary cleft remained ~870 nm and the α-

TABLE I

Morphometric and α-BuTX-binding Density Analyses of Control and Experimental Groups

	No. animals*	No. neuromuscular profiles	Length ratios of 1°cleft:2°cleft: thickened postsynaptic membrane	No. grains	α-BuTX-binding sites μm^2 ± S.E.M. in nmj	Extrajunctional α-BuTX-binding sites/μm^2
Control						
EDL	2	31	1:4.5:1.45	236	19,000 ± 1,290	≤34
SOL	2	23	1:4.5:1.50	189	18,500 ± 970	≤61
Denervated SOL	2	17	1:4.4:1.36	212	16,400 ± 2,500	369 ± 216
Denervated, regenerated SOL	3	27	1:3.9:1.24	270	15,300 ± 3,200	426 ± 190
Regenerated muscle devoid of original MEP	3	32	1:4.5:1.4	348	20,800 ± 1,900	≤64‡

Analysis of variance was used to detect any significant difference in the number of α-BuTX-binding sites/μm^2 in the various groups. At $P < 0.10$, no difference was detected.

nmj, neuromuscular junction.

MEP, motor endplate.

* One muscle was used in each animal.

‡ This density of extrajunctional α-BuTX-binding sites is recorded from myofibers known to be innervated.

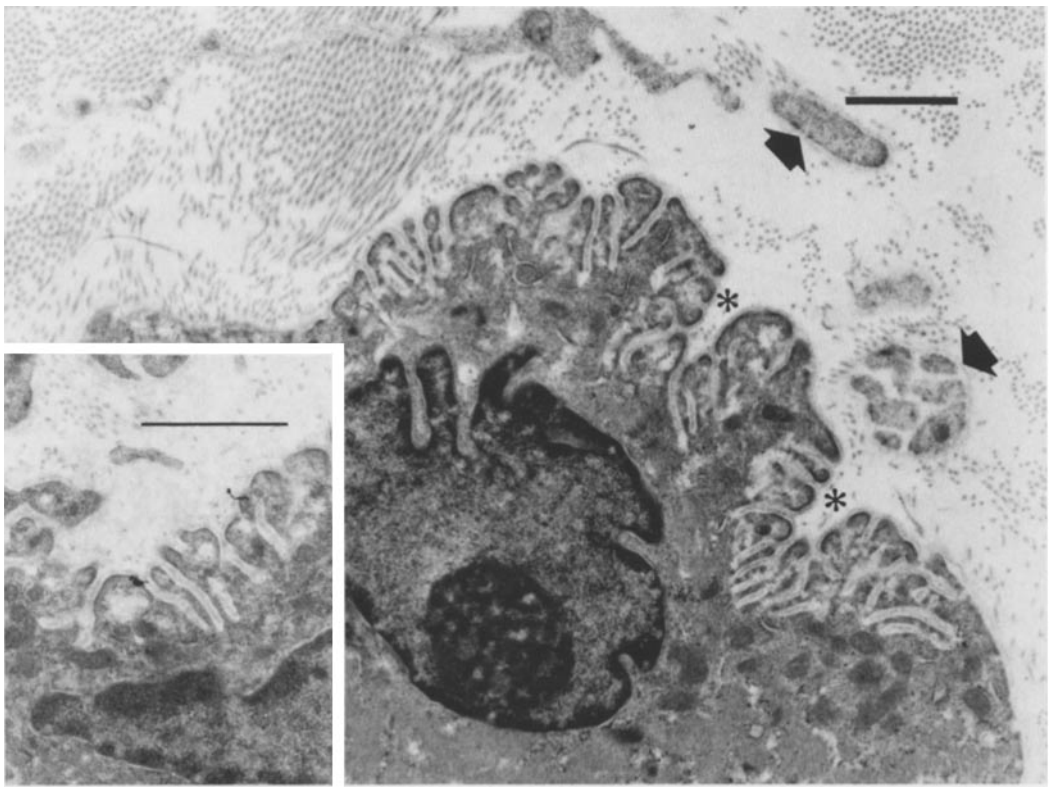

FIGURE 3 Neuromuscular junction of SOL muscle 40 d after denervation. The primary clefts (asterisk) persist after 40 d of denervation although they are somewhat collapsed. Schwann cells (arrows) with their associated basal laminae are present. Uranyl acetate/lead citrate stain. Bar, 1.0 μm. × 12,600. *Inset:* This autoradiogram demonstrates the persistence of α-BuTX-binding sites in denervated SOL muscle 40 d after denervation. Note that the silver grains are located at the top of the secondary clefts. Flat substrate technique, D-19 developer, uranyl acetate/lead citrate stain. Bar, 1.0 μm. × 18,750.

BuTX-binding density was 16,400 sites/μm^2. The density of extrajunctional α-BuTX binding sites in areas near the denervated endplates was 369 sites/μm^2. Previous studies (28, 33) have shown that the density of α-BuTX-binding sites in endplates of denervated myofibers does not decrease during the first 2.5 wk of denervation. By 4–6 wk after denervation, the total number of α-BuTX-binding sites in endplates decreases to 50–70% of control values (17). While this study does not deal with the total number of α-BuTX-binding sites in denervated endplates, from the present study it is apparent that the density of receptors (at least in the area of the thickened postsynaptic membrane) remains at near normal levels. The distribution of α-BuTX-binding sites within denervated SOL endplates, as depicted in Fig. 7, was similar to postsynaptic regions observed in normally innervated muscle and to other studies of AChR distribution in denervated myofibers (33).

Regenerated SOL Muscle in the Absence of Nerve

Detailed studies of the process of skeletal muscle degeneration and regeneration have been published previously (8, 9, 37, 39) and therefore will not be reiterated here.

In 40-d SOL muscle grafts, acetylcholinesterase staining was present only in the area of original endplates at the mid-section of the muscle graft. The diameter of endplates was 29 ± 9 μm. Ultrastructurally, the area of the original endplate could be easily identified by the presence of acetylcholinesterase staining in superficially located myofibers. In deeper areas of the graft where the stain presumably did not penetrate, sites of the original endplate could be identified by the presence of Schwann cells (Fig. 4). These factors suggest, but do not prove, that the regenerated postsynaptic structures are associated with the original endplate. In myofibers that were kept denervated throughout the course of regeneration, the primary clefts appeared most often as grooves in the regenerated myofiber (Fig. 4), but at times the cleft was collapsed on itself. The secondary folds with their associated basal laminae were always present whether the primary cleft was collapsed or not. Thickened postsynaptic membranes were observed at the crests of the synaptic folds (Fig. 4) and the depth of the secondary cleft was 845 nm. In addition, it was of interest to note that myonuclei often were associated with the regenerated but aneural endplates (Fig. 4 and 5) along with Golgi apparatuses, rough endoplasmic reticulum, and mitochondria.

The α-BuTX-binding density for the thickened postsynaptic membrane was found to be 15,300 sites/μm^2, which was not significantly different (as determined by analysis of variance) from the α-BuTX-binding density in endplates of control muscles. Whether the density of α-BuTX-binding sites in nonreinnervated, regenerated myofibers decreases with long periods of time is not known. The distribution of α-BuTX-binding sites within the postsynaptic region of the regenerated myofiber was not significantly different from the distribution of binding sites in denervated myofibers or in the postsynaptic regions of innervated myofibers (Figs. 5 and 7). McMahan and his collaborators (7, 29, 37) have demonstrated that information directing both pre- and postsynaptic differentiation resides in the basal lamina and/or Schwann cells of the original endplate. Whether the same factor(s) leading to the accumulation of AChR also directs the reorganization of AChR in the regenerated postsynaptic structure is not known.

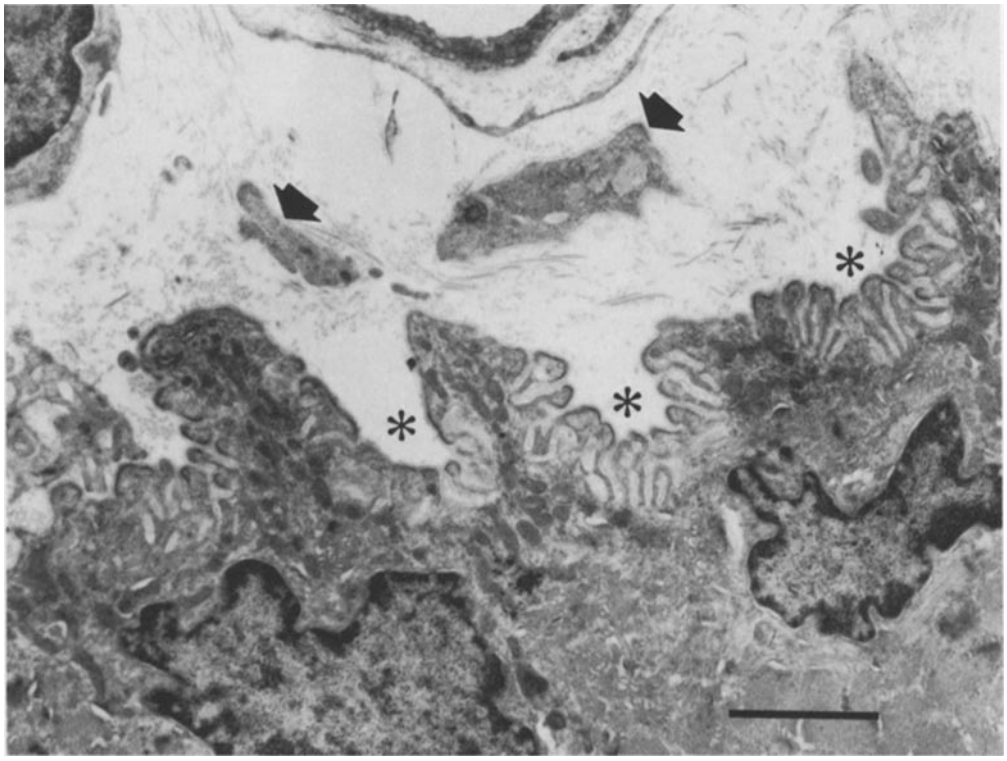

FIGURE 4 40-d SOL muscle regenerate, in the absence of reinnervation. The postsynaptic structure has regenerated even in the absence of the nerve. Primary clefts (asterisk) and secondary clefts are present along with subsynaptic myonuclei. Schwann cells (arrows) with their basal laminae are located above the postsynaptic structures. Uranyl acetate/lead citrate stain. Bar, 1.0 μm. × 18,000.

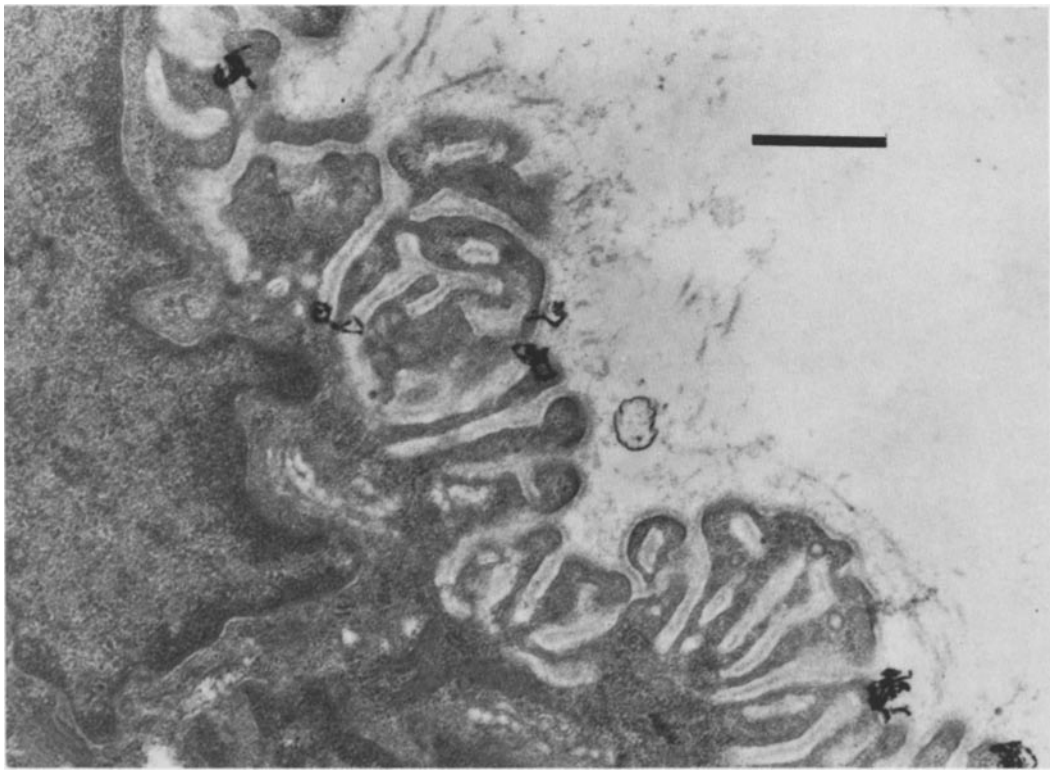

FIGURE 5 Autoradiogram of 40-d SOL muscle regenerate in the absence of the nerve. α-BuTX-binding sites represented by developed silver grains accumulate at the site of the original endplate. Silver grains are located most often at the top of the secondary clefts. Loop technique, D-19 developer, uranyl acetate/lead citrate stain. Bar, 0.5 μm. × 35,000.

FIGURE 6 Autoradiogram of 60-d SOL muscle regenerate devoid of original endplates. This micrograph demonstrates that newly formed endplates have same overall structure as endplates of uninjured muscle (compare with Fig. 2). α-BuTX-binding sites accumulate at these new neuromuscular junctions, and their distribution is similar to the distribution of binding sites in control endplates. Flat substrate technique, Microdol-X developer, uranyl acetate/lead citrate stain. Bar, 1.0 μm. × 26,000.

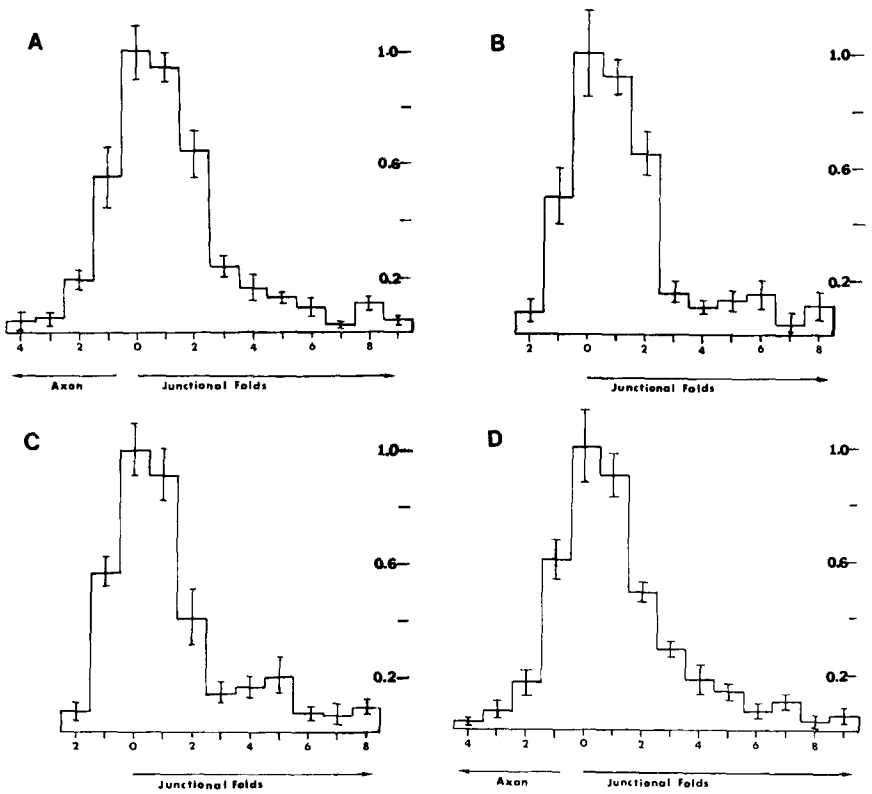

FIGURE 7 Histograms of grain distribution of control and experimental groups. In all cases, only autoradiograms developed with D-19 developer were used. The ordinate is the grain density normalized to 1.0 within each group. The abscissa is divided by HD units (1 HD = 80 nm) and represents the line drawn on the top of the secondary clefts. The grain density at different HD units from the crests of the secondary clefts was determined by counting the number of grain centers and measuring the amount of postsynaptic membrane in that area. The error bars represent sampling error. (*A*) Grain distribution in control EDL endplates (based on 202 grains). This shows that the greatest density of α-BuTX-binding sites is located in the top 200 nm of the secondary clefts. The grain density at the bottom of the clefts drops to low levels. (*B*) Grain distribution in denervated SOL muscle (based on 212 grains). This histogram demonstrates that the distribution of α-BuTX-binding sites remains stable in denervated endplates, although there is a greater density of binding sites at the bottoms of the clefts. (*C*) Grain distribution in regenerated SOL endplates in the absence of the nerve (based on 236 grains). The distribution of grains is very similar to the postsynaptic areas of uninjured muscles. (*D*) Grain distribution in newly formed endplates of regenerated muscle (based on 296 grains). This histogram indicates that the normal distribution of α-BuTX-binding sites is attained in newly formed endplates in regenerated muscle.

Regenerated Muscle Grafts without Original Endplates

Seven 60-d SOL muscle grafts devoid of original endplates were used to count the number of newly formed endplates. These muscles were serially cut in longitudinal section in a cryostat and stained with an AChe/silver stain (1). The average number of newly formed endplates at 60 d was 117 ± 61 endplates/muscle and the diameter of the endplates was 36 ± 22 μm. These endplates were located in the proximal portion of the muscle graft in a position in which no original endplates would be located in an uninjured SOL muscle. This number of newly formed endplates, while greater than previously reported, was still much smaller than the number of endplates formed in SOL grafts with original endplates (1). Previous studies (4, 18, 21, 40) have shown that an undamaged muscle that has had its own nerve severed can be reinnervated by a foreign nerve implant and that ectopic endplates are made primarily in the proximal portion of the muscle near the nerve implant. In one study of reinnervation by a foreign nerve, the number of ectopically formed endplates was found to be 248 ± 51 endplates/muscle (20) while Lømo and Slater (26) have found that 70–100% of the fibers in denervated muscle with foreign innervation were reinnervated by the foreign nerve. It is possible that the connective tissue buildup in muscle grafts (11), the delay in reinnervation of muscle grafts (10 and footnote 1), the lack of original neural pathways, or the variable level of entry of nerves into a free muscle graft may play a role in the reduced number of newly formed endplates seen in the present study.

Ultrastructurally, the newly formed endplates had the highly differentiated appearance of endplates in control muscle. The distance from pre- to postsynaptic membranes was 50 nm and the depth of the secondary clefts was 895 nm (Fig. 6). The length-to-length ratios of the various postsynaptic membrane components were similar to control values (Table I). Although variation occurred, the bottom of the secondary cleft was most often closely apposed to the outermost myofibrils as was observed in endplates of the EDL muscle (compare Figs. 2 and 6). In a study of rat diaphragm, Padykula and Gauthier (32) found that the neuromuscular junction of white myofibers has little sarcoplasmic substance between the bottom of the secondary cleft and the outer surface of the myofibrils, whereas red myofibers have larger cytoplasmic area between the bottom cleft and myofibrils. Korneliussen and Sommerschild (24), in their study of fast nerve implantation into the denervated SOL muscle, have demonstrated that the ectopic endplates formed resemble endplates of fast muscle. In the present study, newly

formed endplates are presumably innervated by axons from the cut nerve to the EDL muscle (a predominantly fast muscle); therefore it would not be unexpected that neuromuscular junctions formed in these muscle grafts would resemble endplates innervated by fast motoneurons.

The density and distribution of AChR within newly formed endplates were not significantly different from those of innervated and uninjured muscle (Fig. 7 and Table I). In myofibers that were known to be innervated, the density of extrajunctional receptors was 64 sites/μm^2. In other myofibers, the density of extrajunctional AChR was greater (~250 sites/μm^2. It is presumed but not proven that this population of myofibers represents noninnervated myofibers.

Thus, while only a relatively small number of newly formed endplates are formed in muscle grafts devoid of original endplates, the organization of these newly formed endplates (e.g., primary and secondary cleft structure, AChR density, and AChR distribution) is not significantly different from that of normally innervated endplates. It appears that factors governing the maintenance of synaptic structure have been established in these ectopic endplates. The previous work of Burden et al. (7) and the present study have shown that factors which mediate the accumulation of AChR are preserved in the site of the original endplate in regenerating muscle. Factors that are located in the basal lamina of the original endplate may be elaborated by the nerve alone or through interaction of the nerve and muscle in regenerating skeletal muscle which is devoid of original endplates. It is plausible that these factors are the same or very similar to factors located in the connective tissue elements of the site of the original endplate.

I would like to thank Professor Bruce M. Carlson for his guidance during this study. Also, I would like to acknowledge the fine work of Mr. John Beckerman, Miss Mary Jo Veasman, and Mrs. Sylvia Goldstein in the preparation of the manuscript.

This research was supported by a National Institutes of Health (NIH) postdoctoral grant (NS06106-02) to David Bader and Muscular Dystrophy Association and NIH (NS06106-02) grants to Bruce M. Carlson.

Received for publication 16 June 1980, and in revised form 17 September 1980.

REFERENCES

1. Bader, D. 1980. Reinnervation of motor endplate-containing and motor endplate-less muscle grafts. *Dev. Biol.* 77:315–327.
2. Barnard, E. A., J. Wieckowski, and T. H. Chiu. 1971. Cholinergic receptor molecules at mouse skeletal muscle junction. *Nature (Lond.).* 234:207–209.
3. Bennett, M. R., T. Florin, and R. Wong. 1974. The formation of synapses in regenerating mammalian striated muscle. *J. Physiol. (Lond.)* 238:79–92.
4. Bennett, M. R., and A. G. Pettigrew. 1976. The formation of neuromuscular synapses. *Cold Spring Harbor Symp. Quant. Biol.* 40:409–424.
5. Berg, D. K., R. B. Kelly, P. B. Sargent, P. Williamson, and Z. W. Hall. 1972. Binding of α-bungarotoxin to acetylcholine receptors in mammalian muscle. *Proc. Natl. Acad. Sci. U. S. A.* 69(1):147–151.
6. Bouteille, M. 1976. The "ligop" method for routine ultrastructural autoradiography. *J. Micro. Biol. Cell.* 27:121–127.
7. Burden, S. J., P. B. Sergent, and U. J. McMahan. 1979. Acetylcholine receptors in regenerating muscle accumulate at original synaptic sites in the absence of the nerve. *J. Cell Biol.* 82:412–425.
8. Carlson, B. M. 1972. The regeneration of skeletal muscle—a review. *Am. J. Anat.* 137: 119–149.
9. Carlson, B. M. 1976. A quantitative study of muscle fiber survival and regeneration in normal, predenervated, and Marcaine-treated free muscle grafts in the rat. *Exp. Neurol.* 52:421–432.
10. Carlson, B. M., K. R. Wagner, and S. R. Max. 1979. Reinnervation of rat extensor digitorum longus muscle after free grafting. *Muscle Nerve.* 2:304–307.
11. Coan, M. R., and R. J. Tomanck. 1980. The growth of regenerating soleus muscle transplants after ablation of the gastrocnemius muscle. *Exp. Neurol.* In press.
12. Fambrough, D. M. 1979. Control of acetylcholine receptors in skeletal muscle. *Physiol. Rev.* 59(1):165–227.
13. Fambrough, D. M., D. C. Drachman, and S. Satyamurti. 1973. Neuromuscular junction in myasthenia gravis: decreased acetylcholine receptors. *Science (Wash. D. C.).* 182:293–295.
14. Fambrough, D. M., and H. C. Hartzell. 1972. Acetylcholine receptors: number and distribution at neuromuscular junctions in rat diaphragm. *Science (Wash. D. C.)* 176:189–191.
15. Fertuck, H. C., and M. M. Salpeter. 1974. Sensitivity in electron microscope autoradiography for ^{125}I. *J. Histochem. Cytochem.* 22:80–87.
16. Fertuck, H. C., and M. M. Salpeter. 1976. Quantitation of junctional and extrajunctional acetylcholine receptors by electron microscope autoradiography after ^{125}I-α-bungarotoxin binding at mouse neuromuscular junctions. *J. Cell. Biol.* 69:144–158.
17. Frank, E., K. Gautvik, and H. Sommerschild. 1976. Persistence of junctional acetylcholine receptors following denervation. *Cold Spring Harbor Symp. Quant. Biol.* 40:275–281.
18. Frank, E., J. K. S. Jansen, T. Lømo, and R. H. Westgaard. 1975. The interaction between foreign and original motor nerves innervating the soleus muscle of rats. *J. Physiol. (Lond.).* 247:725–743.
19. Greenwood, F. C., W. M. Hunter, and J. S. Glover. 1963. The preparation of ^{131}I-labelled human growth hormone of high specific radioactivity. *Biochem. J.* 89:114–123.
20. Gutman, E., and V. Hanzlikova. 1967. Effects of accessory nerve supply to muscle achieved by implantation into muscle during regeneration of its nerve. *Physiol. Bohemoslov.* 16:244–250.
21. Jansen, J. K. S., D. C. Van Essen, and M. C. Brown. 1976. Formation and elimination of synapses in skeletal muscles of rat. *Cold Spring Harbor Symp. Quant. Biol.* 40:425–433.
22. Karnovsky, M. J. 1964. The localization of cholinesterase activity in rat cardiac muscle by electron microscopy. *J. Cell Biol.* 23:217–232.
23. Katz, B., and R. Miledi. 1972. The statistical nature of the acetylcholine potential and its molecular components. *J. Physiol. (Lond.)* 224:665–699.
24. Korneliussen, H., and H. Sommerschild. 1976. Ultrastructure of the new neuromuscular junctions formed during reinnervation of rat soleus muscles by a "foreign" nerve. *Cell Tissue Res.* 167:439–452.
25. Kuffler, S. W., and D. Yoshikami. 1975. The distribution of acetylcholine sensitivity at the postsynaptic membrane of vertebrate skeletal twitch muscles: iontophoretic mapping in the micron range. *J. Physiol. (Lond.)* 244:703–730.
26. Lømo, T., and C. R. Slater. 1978. Control of acetylcholine sensitivity and synapse formation by muscle activity. *J. Physiol. (Lond.)* 275:391–402.
27. Loring, R. E., S. W. Jones, J. Matthews-Bellinger, and M. M. Salpeter. ^{125}I-α-Bungarotoxin: Effects of radiodecomposition on specific activity. *Biochemistry.* In press.
28. Loring, R. H., and M. M. Salpeter. 1980. Denervation increases turnover rate of junctional acetylcholine receptors. *Proc. Natl. Acad. Sci. U. S. A.* 77(4):2293–2297.
29. Marshall, L. M., J. R. Sanes, and U. J. McMahan. 1977. Reinnervation of original synaptic sites on muscle fiber basement membrane after disruption of the muscle cells. *Proc. Natl. Acad. Sci. U. S. A.* 74:3073–3077.
30. Matthews-Bellinger, J., and M. M. Salpeter. 1978. Distribution of acetylcholine receptors at frog neuromuscular junctions with discussion of some physiological implications. *J. Physiol. (Lond.)* 279:197–213.
31. Miledi, R., and L. T. Potter. 1971. The acetylcholine receptors in muscle fibers. *Nature (Lond.).* 233:599–603.
32. Padykula, H. A., and G. F. Gauthier. 1970. The ultrastructure of the neuromuscular junctions of mammalian red, white, and intermediate skeletal muscle fiber. *J. Cell Biol.* 46:27–41.
33. Porter, C. W., and E. A. Barnard. 1975. Distribution and density of cholinergic receptors at the motor endplates of a denervated mouse muscle. *Exp. Neurol.* 48:542–556.
34. Porter, C. W., and E. A. Barnard. 1975. The density of cholinergic receptors at the endplate postsynaptic membrane: Ultrastructural studies in two mammalian species. *J. Membr. Biol.* 20:31–49.
35. Porter, C. W., E. A. Barnard, and T. H. Chiu. 1973. The ultrastructural localization and quantitation of cholinergic receptors at the mouse motor endplate. *J. Membr. Biol.* 14: 383–402.
36. Salpeter, M. M., and L. Bachmann. 1972. Autoradiography. *In* Principles and Techniques of Electron Microscopy. M. A. Hayat, editor. Van Nostrand Reinhold, New York. 2:221–278.
37. Sanes, J. R., L. M. Marshall, and U. J. McMahan. 1978. Reinnervation of muscle fiber basal lamina after removal of myofibers. *J. Cell Biol.* 78:176–198.
38. Thompson, N., A. P. Naftalin, and J. T. Lee. 1978. Experimental study of the role of the motor endplate zone in the transplantation of skeletal muscle autografts in rabbits. *Chic. Plast.* 4(2):81–85.
39. Vracko, R., and E. P. Benditt. 1972. Basal lamina: the scaffold for orderly cell replacement. Observations on regeneration of injured skeletal muscle fibers and capillaries. *J. Cell Biol.* 55:406–419.
40. Waerhaug, O., H. Korneliussen, and H. Sommerschild. 1977. Morphology of motor nerve terminals on rat soleus muscle fibers reinnervated by the original and by a "foreign" nerve. *Anat. Embryol.* 151:1–15.